Original article

Retinazone inhibits certain blood-borne human viruses including Ebola virus Zaire

Andreas J Kesel[1], Zhuhui Huang[2], Michael G Murray[2], Mark N Prichard[3], Laura Caboni[4], Daniel K Nevin[4], Darren Fayne[4], David G Lloyd[4], Mervi A Detorio[5,6], Raymond F Schinazi[5,6]*

[1]Chammünsterstr. 47, Munich, Germany
[2]Southern Research Institute, Frederick, MD, USA
[3]Department of Pediatrics, University of Alabama School of Medicine, Birmingham, AL, USA
[4]Molecular Design Group, School of Biochemistry and Immunology, Trinity College Dublin, Dublin, Ireland
[5]Center for AIDS Research, Laboratory of Biochemical Pharmacology, Department of Pediatrics, Emory University School of Medicine, Atlanta, GA, USA
[6]Veterans Affairs Medical Center, Decatur, GA, USA

*Corresponding author e-mail: andreas.kesel@gmx.de

Background: Human HBV and HIV integrate their retrotranscribed DNA proviruses into the human host genome. Existing antiretroviral drug regimens fail to directly target these intrachromosomal xenogenomes, leading to persistence of viral genetic information. Retinazone (RTZ) constitutes a novel vitamin A-derived (retinoid) thiosemicarbazone derivative with broad-spectrum antiviral activity versus HIV, HCV, varicella-zoster virus and cytomegalovirus.

Methods: The *in vitro* inhibitory action of RTZ on HIV-1 strain LAI, human HBV strain ayw, HCV-1b strain Con1, enhanced green fluorescent protein-expressing Ebola virus Zaire 1976 strain Mayinga, wild-type Ebola virus Zaire 1976 strain Mayinga, human herpesvirus 6B and Kaposi's sarcoma-associated herpesvirus replication was investigated. The binding of RTZ to human glucocorticoid receptor was determined.

Results: RTZ inhibits blood-borne human HBV multiplication *in vitro* by covalent inactivation of intragenic and intraexonic viral glucocorticoid response elements, and, in close analogy, RTZ suppresses HIV-1 multiplication *in vitro*. RTZ disrupts the multiplication of blood-borne human HCV and Ebola Zaire virus at nanomolar concentrations *in vitro*. RTZ has the capacity to bind to human glucocorticoid receptor, to selectively and covalently bind to intraexonic viral glucocorticoid response elements, and thereby to inactivate human genome-integrated proviral DNA of human HBV and HIV.

Conclusions: RTZ represents the first reported antiviral agent capable of eradicating HIV and HBV proviruses from their human host. Furthermore, RTZ represents a potent and efficacious small-molecule *in vitro* inhibitor of Ebola virus Zaire 1976 strain Mayinga replication.

Introduction

Tremendous efforts were initiated to counteract the devastating effect that the blood-borne human viruses, notably HIV, human HBV and human HCV, have on a significant part of the world's population. Approximately 46 million people have died from AIDS-related illnesses since 1981, and 33.3 million individuals (in 2009) were estimated to be currently infected with diverse HIVs [1]. For hepatitis viruses, approximately 370 million (around 6.5% of the world's population) individuals are infected chronically with HBV [2], and 170 million (around 3% of the world's population) individuals are infected chronically with HCV [2]. Infection with the hepatotropic (liver-targeting) *Hepacivirus* (*Flaviviridae*) HCV can result in chronic disease involving liver cirrhosis and/or primary human hepatocellular carcinoma (HCC) [3]. The latter characteristic shares resemblance to the *Orthohepadnavirus* (*Hepadnaviridae*) human HBV, a completely different pathogen which also can manifest itself chronically with progression to HCC [4]. The burden of mortality from viral hepatitis is still increasing, as exemplified in the United States [5]. A clinical challenge is the increasingly high incidence of HIV-1/HBV/HCV triple coinfections [6]. Clearly, a pharmacological agent endowed with simultaneous activity versus HIV-1, HBV and HCV would be highly desirable.

The human herpesvirus 6B (HHV-6B) [7] and the Kaposi's sarcoma-associated herpesvirus (KSHV, human herpesvirus 8 [HHV-8]) [8] are amongst typical blood-borne viral pathogens affecting humans. HHV-8 was recognized as the aetiological agent of Kaposi's sarcoma, a strongly growth factor-dependent neoplastic condition of the skin with high metastatic potential [8]. AIDS-related Kaposi's sarcoma often develops in HIV-1-infected individuals as an opportunistic cancer [8]. HHV-6B, like many other human herpesviruses, causes life-long latent persistence (latency) in its human host, and HHV-6B coinfection is often detected in HIV-1-infected individuals [7]. By analogy, a pharmacological agent endowed with simultaneous activity versus HIV-1, HBV, HCV, HHV-6B and HHV-8 would be most desirable.

Ebola virus (EBOV) was first recognized during the 1976 (northwestern) Zaire (Yambuku, Mongala District, now Democratic Republic of the Congo) epidemic [9]. EBOV 1976 Zaire causes a severe haemorrhagic fever with extremely high mortality (around 90%), and is rated amongst the most hazardous human pathogens [9]. The EBOV 1976 Zaire strain Mayinga is named after Mayinga N'Seka, a nurse who died during the Yambuku outbreak on 20 October 1976. Because fruit bats (*Hypsignathus monstrosus*, *Epomops franqueti* and *Myonycteris torquata*) serve as natural reservoirs of EBOV in equatorial Africa [10], future outbreaks of Ebola haemorrhagic fever are certainly to be expected. A clinically useful, safe and efficacious antiviral agent targeting EBOV would be of major public interest, especially due to the threat of the utilization of EBOV-like viruses as potential bioterrorist attack weapons.

To address these challenges, a vitamin A-derived (retinoid) thiosemicarbazone derivative, retinazone (RTZ; formerly called RTSC-Na 5.5 H_2O; Figure 1A) was prepared from all-*trans* retinyl acetate (vitamin A–acetate) by chemical synthesis [11] and proved to exhibit broad-spectrum antiviral activity [11] including the viruses HIV type-1 strain LAI (HIV-1_{LAI}) [12], HCV subtype 1b strain Con1 (HCV-1b Con1) [13], human varicella-zoster virus (VZV, human herpesvirus 3 [HHV-3] strain Ellen), and human cytomegalovirus (HCMV, human herpesvirus 5 [HHV-5] strain AD169). New data indicated suppressing activity of RTZ on enhanced green fluorescent protein (eGFP)-expressing Ebola virus Zaire (eGFP–EBOV Zaire 1976 strain Mayinga [14]) multiplication, on wild-type Ebola virus Zaire (EBOV Zaire 1976 strain Mayinga) virus yield, on human herpesvirus 6B (HHV-6B strain Z29) replication and on Kaposi's sarcoma-associated herpesvirus (HHV-8 strain BCBL-1) production from latency.

Materials and methods

Materials

The synthesis and the analytical data of RTZ were reported previously [11]. Chemicals were of analytical or best available quality. 1,2-Phenylenediamine was purchased from Merck–Schuchardt OHG (Hohenbrunn, Germany). Vitamin A–acetate (purity 95%) oily concentrate (approximately 0.327 g all-*trans* retinyl acetate/g oil) and glacial acetic acid (HOAc) 100% *pro analysi* were purchased from AppliChem GmbH (Darmstadt, Germany). Hydrocortisone micronized Ph.Eur. 6.5 was purchased from Caelo (Caesar & Loretz GmbH, Hilden, Germany). The lambda (λ) bacteriophage λ*c*I*ts*857 *ind*1 *S*am7 [15] double-stranded DNA (dsDNA; 5 A_{260} units, 0.25 µg/µl in 10 mM Tris–HCl [pH 8.0] +1 mM EDTA [TE buffer]; 1,000 µl) was from Roche Diagnostics Deutschland GmbH (Roche Applied Science, formerly Boehringer Mannheim GmbH, Mannheim, Germany). The 48,502 bp (32,300 kDa) λ dsDNA with *cos* sticky ends carries the following mutations in comparison to wild-type λ virus: 37,589 C→T (*ind*1); 37,742 C→T (*c*I857); 43,082 G→A (*ts*); 45,352 G→A (*S*am7). The temperature (70°C) for the experiment in *Covalent modification of* λ *DNA by RTZ* in Additional file 1 was selected 10 K below the reported melting temperature (80°C) of λ*c*I*ts*857 *ind*1 *S*am7 dsDNA [16]. The analysis of the *cos* (cohesive sticky ends) oligomer composition of λ dsDNA was published [17].

Virology

HIV-1 replication reverse transcriptase assay

HIV-1_{LAI} (=HIV-1_{BRU} =LAV-1) was assayed in primary human peripheral blood lymphocyte (PBL) cells in the presence of a drug being evaluated. The parameter for antiviral activity was reduction of reverse transcriptase (RT) activity in the cell supernatant after Triton X–100-mediated lysis of released virions, as measured by [5α-^{3}H]dTTP (5α-tritiated thymidine 5′-triphosphate) incorporation into poly(rA) • poly(dT) directed by the primed RNA template poly(rA) • oligo(dT). It should be noted that the assay did not detect RT inhibition by potential RT inhibitors *per se*, but indirectly quantified the amount of released HIV-1 in the supernatant. The detailed assay methodology was reported by Schinazi *et al*. [18], as based on an older assay system of Spira *et al*. [19]. The experiments were conducted in triplicate and treated statistically by regression curve analysis (r^2 coefficient of determination). The RT inhibitor zidovudine (AZT, 3′-azido-3′-deoxythymidine; RETROVIR™) served as a positive control. Cytotoxicity on PBL cells exerted by the test compounds was determined as described by Stuyver *et al*. [20], by application of the CellTiter 96® AQ_{ueous} One Solution Cell Proliferation Assay (Promega Corp., Madison, WI, USA). Briefly,

Figure 1. Chemical structure of RTZ

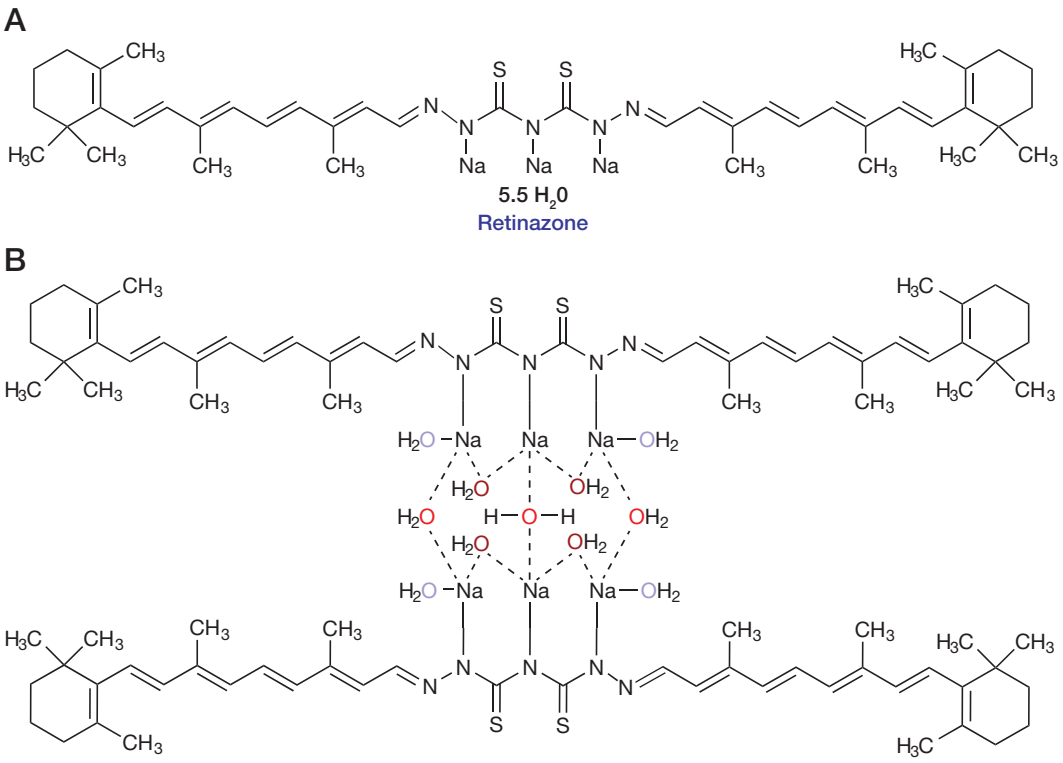

(A) Retinoid dimer formula (M=863.11 g/mol) as trisodium salt hemihendecahydrate (×5.5 H_2O). For all biological evaluations this formula was applied. **(B)** Dimer-of-a-dimer sodium hydrate coordination complex formula (M=1,726.22 g/mol) of retinazone (RTZ) showing the tetrahedral sodium hydrate cluster (×11 H_2O, hendecahydrate). **(C)** Perspective view of the three-dimensional arrangement of the tetrahedral sodium hydrate cluster $[Na_6(H_2O)_{11}]^{6+}$ contained in RTZ [11]. This sodium hydrate cluster could be compared to an octahedral sodium hydrate cluster hydrate $[Na_2(H_2O)_{11}]^{2+}\times 6\ H_2O$ [40].

the phenazine ethosulfate (PES)-coupled reduction of the tetrazolium salt 3-(4,5-dimethylthiazol-2-yl)-5-(3-carboxymethoxyphenyl)-2-(4-sulfophenyl)-2*H*-tetrazolium (MTS) to a purple, water-soluble formazan by living, undamaged cells was measured.

Extracellular (virion) HBV ayw DNA dot blot hybridization assay

The general assay methodology was described previously [21,22]. The assays were conducted in HepG2 2.2.15 HBV ayw producer HCC cell line, harbouring a persistently human chromosome-integrated HBV ayw genome, which was cultured as described previously [21,22]. Briefly, after isolation of HBV DNA [21], extracellular (virion) HBV ayw episomal covalently closed circular (cccDNA) levels were assessed by quantitative dot blot hybridization. The probe used was a gel-purified, restriction endonuclease *Eco*RI-digested (linearized) HBV ayw DNA 3.2 kb (3,182 bp) fragment [23], which was phosphorus-32 (^{32}P)-labelled by DNA polymerase I-mediated nick translation with [α-^{32}P]dCTP ([α-^{32}P]-2'-deoxycytidine 5'-triphosphate). The relative quantification of the ^{32}P signal hybridized to the sample was compared to the signal hybridizing to known quantities of HBV ayw DNA standards, as included with each nitrocellulose filter (dot blot). Standard curves, generated by multiple positive control analyses, were used to correlate relative counts-per-minute (cpm) measurements with standard HBV ayw DNA cpm. Host cellular (HepG2 2.2.15) toxicity was determined by neutral red lysosomal uptake assay as described previously [21,22].

Extracellular (virion) HBV ayw DNA TaqMan® RT-qPCR assay

The general TaqMan® RT-qPCR assay methodology was described previously as liver HBV DNA assay [24]. The anti-HBV assay developed at Southern Research Institute employs real-time quantitative PCR (RT-qPCR, TaqMan®) to directly measure extracellular HBV DNA copy number. Briefly, HepG2 2.2.15 cells were plated in 96-well microtitre plates. On the following day, the HepG2 2.2.15 cells were washed and the medium was replaced with complete medium containing various concentrations of a test compound in triplicate. The antiretroviral drug (–)-lamivudine (3′-thia-2′,3′-dideoxy-L-cytidine, 3TC; EPIVIR™, ZEFFIX™) was used as the positive control, while medium alone was added to cells as a negative control (virus control). Three days later, the culture medium was replaced with fresh medium containing the appropriately diluted drug. Six days following the initial administration of the test compound, the cell culture supernatant was collected, treated with pronase, and then used in a TaqMan® RT-qPCR assay to determine HBV DNA copy numbers. The fluorescent dye (6-FAM)/quencher dye (TAMRA)-labelled TaqMan® RT-qPCR probe utilized spanned from nt 2,333 to nt 2,363 of HBV ayw DNA and was composed of and labelled with: 5′-(6-FAM)–CGGAAACTACTGTTGTTAGACGACGAGGCAG–(TAMRA–[6-FAM])-3′ ([6-FAM] = 6-carboxyfluorescein; TAMRA = 6-carboxytetramethylrhodamine). The forward primer spanned from nt 2,305 to nt 2,325 of HBV ayw DNA: 5′-CCAAATGCCCCTATCCTATCA-3′. The reverse primer spanned from nt 2,392 to nt 2,370 of HBV ayw DNA: 5′-GAGGCGAGGGAGTTCTTCTTCTA-3′. FullVelocity™ quantitative PCR (qPCR) Master Mix (Stratagene, Inc., La Jolla, CA, USA) was used. The assay was run with a series of dilutions of DNA isolated from HepG2 2.2.15 cells to obtain a standard curve, with the *x*-axis as the threshold cycle (C_T) value, and the *y*-axis as the $\log_{10}$ dilution of the standard. Obtained r^2 values were used to measure the quality of the curve and, deduced from it, the efficiency of the TaqMan® RT-qPCR. The r^2 regression curve correlation values were always above 0.98 (the average r^2 value of the TaqMan® RT-qPCR procedure was 0.99). Mean C_T values were obtained for duplicates of each sample. The mean C_T values of each sample were used to obtain the relative $\log_{10}$ DNA value by using a formula of the fit line of the standard curve. Antiviral activity was calculated from the reduction in HBV DNA levels relative to the controls. The cells were used to assess cytotoxicity 50% with CellTiter 96® AQ_{ueous} One Solution Cell Proliferation Assay (MTS) kit (Promega) according to manufacturer's protocol.

HCV Huh7 ET (luc-ubi-neo/ET) replicon

The anti-HCV activity of RTZ was assessed using a subgenomic HCV replicon. The Huh7 ET cell line was kindly provided by Ralf Bartenschlager (Department of Molecular Virology, University of Heidelberg, Heidelberg, Germany) [25,26]. The ET cell line is a human HCC cell line (derived from Huh7) that contains a Con1 (genotype 1b) bicistronic subgenomic replicon. The subgenomic replicon contains a stable luciferase reporter gene, three cell culture-adaptive mutations (E1202G, T1280I, K1846T; numbered according to GenBank accession number AJ238799.1 [HCV-1b Con1 complete genome, 9,605 bp]) [26], the genuine HCV-1b internal ribosomal entry site (IRES), and the first amino acid codons of the HCV core protein which drive the production of luciferase, ubiquitin and neomycin phosphotransferase fusion protein. The murine encephalomyocarditis virus (EMCV, *Picornaviridae*, *Cardiovirus*) IRES element directs the translation of the second cistronic unit which encodes the non-structural proteins NS3, NS4A, NS4B, NS5A and NS5B. Cells were grown in Dulbecco's modified essential medium (DMEM) with 10% fetal bovine serum (FBS), 1% penicillin–streptomycin, 1% L-glutamine, 1% non-essential amino acids and 250 µg/ml G418 (geneticin) in a 5% CO_2 incubator at 37°C.

HCV Huh7 ET (luc-ubi-neo/ET) replicon luciferase reporter assay

The general assay methodology was described previously [27,28]. Assessments of antiviral activity and cytotoxicity were carried out in parallel in clear-bottomed 96-well plates according to Southern Research Institute's standard format. The reporter replicon cells were seeded into two identical sets of 96-well plates at a density of 5×10^3 cells per well in 0.1 ml of DMEM without selection antibiotic (G418) in a humidified atmosphere supplemented with 5% CO_2 at 37°C. RTZ was initially solubilized in DMSO. Half-$\log_{10}$ serial dilutions of RTZ, typically spanning the range of 63 nM to 20 µM, were then prepared in DMEM +5% FBS and then applied to the corresponding wells. Human recombinant interferon-α2b (PBL Biomedical Laboratories, New Brunswick, NJ, USA) was included as a positive control at half-$\log_{10}$ dilutions in DMEM typically spanning the range of 0.006 to 2.0 IU/ml. Following 72 h incubation, one set of the cells was processed to assess the replicon-derived luciferase activity with the Steady-Glo® Luciferase Assay System (Promega) according to manufacturer's instructions. The activity of the luciferase reporter is proportional to HCV-1b Con1 RNA levels. The percent inhibition was plotted against the nominal concentration of compound to derive values for effective inhibitory concentration 50% (EC_{50}). Cytotoxicity in the subgenomic replicon assay was assessed by using the CytoTox-ONE™ Homogeneous Membrane Integrity Assay Kit (Promega). The CytoTox-ONE™ Assay is a rapid, fluorescent measurement of the release of lactate dehydrogenase (LDH) from cells with a damaged membrane. LDH released into the culture medium is measured with a 10 min coupled enzymatic assay that results in the conversion of resazurin into resorufin in the presence of diaphorase. The CytoTox-ONE™ Reagent mix does not damage healthy cells; therefore the reactions to measure released LDH can be performed directly in a homogeneous format in assay wells containing a mixed population of viable and damaged cells.

HCV Huh7 ET (luc-ubi-neo/ET) replicon TaqMan® RT-qPCR assay

The general assay methodology was described previously [27,28]. The cell culture conditions were identical to the luciferase reporter assay. Cells were processed after a 72-h incubation at 37°C. The diluted compounds were applied to appropriate wells in the 96-well plates. Human recombinant interferon-α2b (PBL Biomedical Laboratories) was included as a positive control. The intracellular RNA from each well was extracted using the RNeasy® 96 Kit (Qiagen, Inc., Valencia, CA, USA). The level of HCV RNA was determined by a real-time reverse transcriptase PCR assay using TaqMan® One-Step RT-qPCR Master Mix Reagents (Applied Biosystems, Foster City, CA, USA) and an ABI PRISM® 7900 sequence detection system (Applied Biosystems). The cytotoxic effects were measured with TaqMan® Ribosomal RNA Control Reagents (Applied Biosystems) as an indication of cell numbers. The amounts of HCV RNA and ribosomal RNA (rRNA) were then plotted into Southern Research Institute's antiviral evaluation format to derive the EC_{50} and cytotoxic concentration 50% (CC_{50}).

eGFP–EBOV Zaire 1976 Mayinga antiviral assay

The general assay methodology was described previously [29]. EBOV Zaire 1976 Mayinga expressing the eGFP was derived by reverse genetics to generate a full-length cDNA clone inserted with a foreign reporter gene eGFP (eGFP–EBOV Zaire 1976 Mayinga) [14]. Vero E6 cells (VERO C1008; Vero 76, clone E6) were seeded at 4×10^4 cells/well (100 µl) in black 96-well plates and incubated at 37°C and 5% CO_2 with Eagle's minimum essential medium (EMEM; Invitrogen™/Life Technologies™, Carlsbad, CA, USA) complete with 10% FBS +5% L-glutamine and HEPES buffer (EMEM–C). After 24-h incubation of seeded cells, and proper dilution of the compounds dissolved in DMSO with EMEM, a suitable amount of test compound (4× concentrated, 50 µl) from the dilution plate was transferred to two cell plates; one cell plate was used for the eGFP–EBOV Zaire 1976 Mayinga infection and the second for the cytotoxicity assay. The plates used for the eGFP–EBOV Zaire 1976 Mayinga infection were transferred into Bio-Safety Level (BSL)-4 containment, whereas those used for the cytotoxicity assay remained at BSL-2 containment until the 48 h time point. At BSL-4, 50 µl of eGFP–EBOV Zaire 1976 Mayinga virus diluted in EMEM was added to each infection plate at a multiplicity-of-infection (MOI) of 1. Infected eGFP–EBOV Zaire 1976 Mayinga assay plates incubated for 48 h at 37°C and 5% CO_2; after incubation, plates were read for eGFP fluorescence (excitation 485 nm, emission 515 nm, cutoff 495 nm; 6 reads/well) on a Gemini™ EM spectrofluorometer (Molecular Devices, Sunnyvale, CA, USA). At the same time, plates remaining in BSL-2 were used for the cytotoxicity assay. The RTZ experiment was run in triplicate and treated statistically by Kruskal–Wallis one-way analysis of variance (ANOVA) on ranks with Bonferroni correction post-test (as compared to the associated virus control). Internal controls were +cells/+virus/-RTZ and +cells/-virus/-RTZ. The effect of RTZ on eGFP–EBOV Zaire 1976 Mayinga multiplication was expressed as a percentage of these controls and plotted against the RTZ concentration.

eGFP–EBOV Zaire 1976 Mayinga cytotoxicity assay

The CellTiter–Glo® Luminescent Cell Viability Assay (Promega) is a method of determining the number of viable cells based on the quantitation of adenosine 5′-triphosphate (ATP) with ATP-dependent Ultra–Glo™ Recombinant Luciferase (from the firefly

Photuris pennsylvanica), which is an indirect quantification of the state of metabolically active cells (Promega). CellTiter–Glo® Buffer and lyophilized CellTiter–Glo® Substrate were removed from -20°C storage into -4°C for thawing 24 h before use. After proper thawing and equilibration to room temperature, the CellTiter–Glo® buffer (100 ml) was added to the CellTiter–Glo® Substrate and mixed by inverting the closed amber bottle to reconstitute the lyophilized enzyme/substrate mixture, making the CellTiter–Glo® Reagent mixture. All media and compound concentrations added to the assay plate (200 µl), as described before, were discarded by flicking into a waste container after 48 h incubation with compounds. CellTiter–Glo® reagent mixture (100 µl) and DMEM (Invitrogen™/Life Technologies™; 100 µl) were added. After addition of the reagent and media, the samples were mixed using an orbital shaker for 2 min; after mixing, plates were incubated at room temperature for 10 min to stabilize the luminescence signal. Plates were then read for fluorescence (excitation 485 nm, emission 515 nm, cutoff 495 nm; 6 reads/well) on a Gemini™ EM spectrofluorometer (Molecular Devices).

EBOV Zaire 1976 Mayinga (wild-type) antiviral assay

The assay was performed in Vero cells with wild-type EBOV Zaire 1976 Mayinga virus as described previously [30]. The utilized positive control drug was the guanine nucleobase antimetabolite 3-deazaguanine (6-amino-1,5-dihydro-4*H*-imidazo[4,5-*c*]pyridin-4-one, 3-DG) [31]. The applied assay method was the determination of virus yield reduction (VYR) utilizing crystal violet staining. The VYR assay determines actual virus yield in the presence and absence of the test compound; this is the confirmatory assay for antiviral activity. The effective concentration 90% (EC_{90}) was determined by VYR for both 3-deazaguanine and RTZ. The cytotoxicity 50% exerted on Vero cells by both 3-deazaguanine and RTZ was determined by neutral red lysosomal uptake cell viability assay [32].

HHV-6B Z29 DNA hybridization assay

The general assay methodology was described previously [33,34]. In detail, uninfected MOLT-3 cells were added to 96-well plates at a concentration of 1×10^4 cells/well. Infection was initiated by adding HHV-6B-infected MOLT-3 cells at a ratio of approximately 1 infected cell for every 10 uninfected MOLT-3 cells. Drugs were serially diluted and added to triplicate wells. The anti-DNA-viral agent cidofovir (1-[(2*S*)-3-hydroxy-2-(phosphonomethoxy)-1-propyl]-1*H*-cytosine, CDV; VISTIDE™) was included as positive control. Drug-free medium was added to the wells that contained the cell and virus controls. The plates were incubated for seven days at 37°C. After incubation, 100 µl of 3× denaturation buffer (4.5 M NaCl, 1.2 M NaOH) was added to each well, and 50 µl was added to the wells of a Bio-Dot® apparatus (Bio-Rad Laboratories, Inc., Hercules, CA, USA) containing an Immobilon™ nylon membrane (Millipore, Bedford, MA, USA). A 50-µl aliquot of denatured DNA from the infected cells was aspirated through the membrane, and then 50 µl of denaturation buffer and 50 µl of phosphate-buffered saline (PBS) were added. The membrane was allowed to air dry, equilibrated in 2×SSC (1×SSC is 0.15 M NaCl plus 15 µM sodium citrate)–0.1% (m/v) sodium dodecyl sulfate (SDS), and prehybridized in DIG Easy Hyb (Roche Applied Science, Indianapolis, IN, USA) for 30 min at 37°C. A specific HHV-6A digoxigenin (DIG)-labelled probe was prepared by PCR (Roche Applied Science) from HHV-6A strain U1102 DNA using suitable primers. The forward primer spanned from nt 37,820 to nt 37,839 of HHV-6A strain U1102 DNA (GenBank accession number X83413.1): 5′-TGGGATTGGGATTAGAGCTG-3′. This HHV-6A forward primer corresponds to HHV-6B strain Z29 DNA from nt 38,936 to nt 38,955: 5′-GTCTCTTAGGATTGGAGCTG-3′. The reverse primer spanned from nt 38,418 to nt 38,399 of HHV-6A strain U1102 DNA: 5′-CCTTGATCATTCGACCGTTT-3′. This HHV-6A reverse primer is identical to HHV-6B strain Z29 DNA from nt 39,534 to nt 39,515. Therefore, a segment from nt 38,936 to nt 39,534 of HHV-6B strain Z29 DNA was detected by the HHV-6A strain U1102 probe. This fragment is located in the U27 gene coding for polymerase processivity factor (NCBI Reference Sequence accession number NC_000898.1). The denatured probe was allowed to hybridize to the viral DNA on the filter overnight at 37°C. The membrane was washed once at 37°C with 2×SSC–0.1% SDS, three times with 0.2×SSC–0.1% SDS, and once with 0.1×SSC–0.1% SDS. Detection of specifically bound DIG probe was performed with anti-DIG antibody using the manufacturer's protocol (Roche). An image of the film was captured digitally and quantified with Quantity One® software (Bio-Rad), and EC_{50} values were calculated as previously described [33]. CC_{50} was evaluated by application of the CellTiter–Glo® Luminescent Cell Viability Assay (Promega) as previously described [35,36].

HHV-8 BCBL-1 DNA TaqMan® RT-qPCR assay

Antiviral activity against HHV-8 was evaluated by methods reported previously in concise form [37]. In detail, BCBL-1 cells (NIH, NIAID, Division of AIDS, AIDS Research and Reference Reagent Program, Germantown, MD, USA) were maintained in growth medium consisting of RPMI 1640 supplemented with 10% FBS, penicillin, gentamicin, and L-glutamine, and 2×10^4 cells were added to each well in a 96-well plate. Compounds were diluted in triplicate wells of a 96-well plate, with the highest dilution yielding a concentration of 60 µM.

The anti-DNA-viral agent cidofovir was included as positive control. The BCBL-1 cells were induced to undergo a lytic infection by the addition of phorbol 12-myristate 13-acetate (Promega) at a final concentration of 100 ng/ml. Plates were incubated for 7 days at 37°C in a humidified CO_2 incubator. Total DNA was prepared with a Wizard® SV 96 Genomic DNA Purification System 96-well purification kit (Promega), and viral DNA was quantified by TaqMan® RT-qPCR. The fluorescent dye (6-FAM)/quencher dye (TAMRA)-labelled TaqMan® RT-qPCR probe utilized spanned from nt 14,144 to nt 14,160 of HHV-8 GK18 DNA and was composed of and labelled with: 5′-(6-FAM)–CCTACGTGTTCGTCGAC–(TAMRA)-3′. The forward primer spanned from nt 14,120 to nt 14,142 of HHV-8 GK18 DNA: 5′-TTCCCCAGATACACGACAGAATC-3′. The reverse primer spanned from nt 14,182 to nt 14,166 of HHV-8 GK18 DNA: 5′-CGGAGCGCAGGCTACCT-3′. Plasmid pMP218 containing a DNA sequence corresponding to nt 14,120 to nt 14,182 (HHV-8 GK18, GenBank accession number AF148805.2) was used to provide absolute quantification of viral DNA. Compound concentrations sufficient to reduce viral DNA accumulation by 50% (EC_{50}) were calculated by standard methods. CC_{50} was evaluated in a duplicate plate containing BCBL-1 cells with the same exposure as to the test compounds by application of the CellTiter–Glo® Luminescent Cell Viability Assay (Promega) as previously described [35,36].

Cell biology

LanthaScreen® TR–FRET glucocorticoid receptor coactivator assay

The LanthaScreen® time-resolved Förster (fluorescence) resonance energy transfer (TR–FRET) glucocorticoid receptor coactivator assay (Invitrogen™/Life Technologies™) is based on quantifying the binding of the fluorescein-labelled coactivator peptide SRC1–4 (19-mer C-terminal part of steroid receptor coactivator-1 [SRC-1] [38], aa 1,423–1,441 [GPQTPQAQQKSL**LQQLL**TE, with nuclear receptor interaction motif 4, the NR box 4, in bold and underlined] of NCBI Reference Sequence NP_003734.3) to a glutathione *S*-transferase (GST) fusion protein (expressed in insect cells; 57.6 kDa) with human glucocorticoid receptor isoform α (hGRα) ligand-binding domain (LBD; aa 521–777 of NCBI Reference Sequence NP_000167.1) by TR–FRET utilizing a sensitized terbium (Tb^{3+})-chelate-labelled anti-GST antibody (150 kDa). Briefly, this assay serves for qualitative discrimination whether a test compound represents an agonist or an antagonist at hGRα, exploiting that coactivator peptide binding to hGRα is strictly agonist-dependent [38]. The assay was run both in agonist and antagonist mode according to manufacturer's instructions by detecting the fluorescence emission ratio 520 nm (fluorescein emission)/495 nm (sensitized Tb^{3+}-chelate emission). The higher this ratio is measured, the more SRC1–4 is bound to hGRα LBD. In agonist mode the potential enhancement of the binding of SRC1–4 to hGRα LBD (an indirect indication of agonist activity) by RTZ was monitored to assess if RTZ incorporates agonist activity at hGRα LBD. In antagonist mode the hGRα antagonist mifepristone (RU-38486, RU486; 11β-[4-(dimethylamino) phenyl]-17β-hydroxy-17α-(1-propynyl)estra-4,9(10)-dien-3-one; MIFEGYNE™) [39] was used at a fixed concentration of 100 µM serving as control suppressing the 520 nm/495 nm fluorescence emission ratio by displacing the agonist dexamethasone (and, as a consequence, SRC1–4) from hGRα LBD. RTZ was assayed in antagonist mode at the concentrations of 10 µM, 50 µM and 100 µM. These high concentrations were selected to have total comparability at maximal displacement of the agonist within the antagonist assay experiment. In detail, TR–FRET values were calculated at 10 flashes per well, using a delay time of 100 µs and integration time of 200 µs as recommended by the Invitrogen assay guidelines. The TR–FRET signal was measured with PHERAstar *Plus* equipment (BMG LABTECH GmbH, Ortenberg, Germany) using a LanthaScreen® optic module (excitation 335 nm, emission 520 nm [channel A] and 495 nm [channel B]). The ratio 520 nm/495 nm was then calculated and plotted against compound concentration. A serial dilution of compounds was prepared in 100×DMSO starting from the maximum desired concentration. Each 100× solution was diluted to 2× concentration with TR–FRET nuclear receptor buffer F (pH 7.5, containing 10% glycerol, exact composition not disclosed by Invitrogen™/Life Technologies™), yielding a final concentration of 1% (v/v) DMSO in each well. A volume of 10 µl of 2× solution was added to a black low volume 384-well assay plate (Corning, Inc., Corning, NY, USA), followed by addition of 5 µl 4×hGRα LBD (10 mM potassium phosphate pH 7.4, 0.1 mM EDTA, 10 mM Na_2MoO_4, 5 mM 1,4-dithiothreitol [DTT], 20% glycerol) and 5 µl of fluorescein-SRC1–4 (100 µM in 25 mM HEPES pH 7.5, with 50% [v/v] DMSO)/Tb^{3+}-chelate-labelled anti-GST antibody (in HEPES-buffered saline which is 137 mM NaCl, 2.7 mM KCl, 10 mM HEPES pH 7.5) in agonist mode. Antagonist mode was run using 5 µl 4×hGRα LBD and 5 µl fluorescein-SRC1–4/Tb^{3+}-chelate-labelled anti-GST antibody/4× dexamethasone (included at a concentration equal to EC_{80}, which was determined by running the assay in agonist mode first: EC_{80}=10^{(logEC_{50})+[(1/Hill slope)×log(80/100-80)]}=773 nM). Fluorescein-SRC1–4 and sensitized Tb^{3+}-chelate-labelled anti-GST antibody were premixed in light protecting vials prior to use. The final concentration of 5 mM DTT was used in the assay buffer in order to prevent protein degradation. Plates were incubated at room temperature and

protected from light prior to measurement. In line with the assay protocol, an agonist (dexamethasone) or an antagonist (RU486), respectively, was used as positive control. A control with no hGRα LBD present was included to account for diffusion-enhanced FRET or ligand-independent coactivator recruitment. A negative control with 2×DMSO (replacing test compound) was present to account for any solvent vehicle effects. All experiments were run in triplicate and treated statistically by two-way analysis of variance (ANOVA) with Bonferroni correction post-test (as compared to the associated vehicle control).

LanthaScreen® TR–FRET glucocorticoid receptor competitive binding assay

The LanthaScreen® TR–FRET glucocorticoid receptor competitive binding assay (Invitrogen™/Life Technologies™) is based on monitoring the competitive displacement (by an agonist or antagonist) of the fluorescein-labelled glucocorticoid agonist Fluormone™ GS1 Green (exact structure not disclosed by Invitrogen™/Life Technologies™) from a GST fusion protein with hGRα LBD by TR–FRET utilizing a sensitized Tb^{3+}-chelate-labelled anti-GST antibody. All general conditions were identical to the coactivator assay. A serial dilution of compounds was prepared in 100×DMSO, starting from the maximum desired concentration which was 200 µM for RTZ. Each 100× solution was diluted to 2× concentration with TR–FRET nuclear receptor buffer F, yielding a final concentration of 1% (v/v) DMSO in each well. A volume of 10 µl of 2× solution was added to a black low volume 384-well assay plate (Corning), followed by addition of 5 µl 4×hGRα LBD/Tb^{3+}-chelate-labelled anti-GST antibody and 5 µl of 4× (80 nM) Fluormone™ GS1 Green (25× stock solution is 500 nM in 75% [v/v] aqueous methanol, to be diluted to 4× with TR–FRET nuclear receptor buffer F). Dexamethasone was included as a positive control at the high concentration of 20 µM, securing 100% Fluormone™ GS1 Green displacement from hGRα LBD. A negative control with 2×DMSO was present to account for any solvent vehicle effects. The hGRα LBD and the sensitized Tb^{3+}-chelate-labelled anti-GST antibody were premixed in light protecting vials prior to use. The final concentrations of 5 mM DTT and of 1×hGRα-stabilizing peptide (10×hGRα-stabilizing peptide is 1 mM in 10 mM potassium phosphate pH 7.4, exact identity not disclosed by Invitrogen™/Life Technologies™) were used in the assay buffer in order to prevent protein degradation. Plates were incubated at room temperature protected from light for 2 hours prior to TR–FRET measurement. The vehicle control was set as 0% Fluormone™ GS1 Green agonist displacement from hGRα LBD, and the 20 µM dexamethasone experiment was treated as 100% Fluormone™ GS1 Green agonist displacement from hGRα LBD. The percentage values of agonist displacement from the hGRα LBD by RTZ were calculated in relation to these control values from the TR–FRET signal ratios 520 nm/495 nm, and were plotted against the logarithmic (log_{10}) RTZ concentrations. All experiments were run in triplicate and treated statistically by two-way analysis of variance (ANOVA) with Bonferroni correction post-test (as compared to the associated vehicle control).

Results

The chemical structure of RTZ and its purity

The chemical structure of RTZ was elucidated as retinoid dimer-of-a-dimer sodium hydrate coordination complex [11] (Figure 1B and 1C), as based on prior experiences with structurally related sodium hydrate clusters [40]. RTZ was synthesized in ≥98% (n/n) purity according to proton nuclear magnetic resonance (^{1}H NMR) spectroscopy (*700.430 MHz proton nuclear magnetic resonance [^{1}H NMR] spectrum of RTZ dissolved in DMSO-d_6* in Additional file 1). RTZ is a remarkably stable compound, despite containing a retinoid polyene, due to intramolecular cessation of oxygen-initiated radical chain reactions by the intrinsic sulfur content. An impurity of RTZ, the content of which was diminished during purification in concentration, the so-called OBH acetate, was synthesized independently from vitamin A–acetate in the form of OBH chloride hydrate. The structure of OBH chloride hydrate was elucidated by NMR spectroscopy (*700.430 MHz proton nuclear magnetic resonance [^{1}H NMR] spectra of OBH chloride×1/3 H_2O* in Additional file 1) as stable cyclic oxonium salt retaining the vitamin A diterpenoid (C_{20}) carbon scaffold. Its structure was verified unequivocally by independent synthesis as stable cyclic oxonium salt OBH chloride×1/3 H_2O, similar in structure to the recently reported cyclic oxonium salts oxatriquinane [41] and 1,4,7-trimethyloxatriquinane [42]. OBH chloride hydrate was non-toxic to cultured cells (CEM and Vero cells, respectively: CC_{50}>100 µM) and did not exhibit antiviral activity against HIV-1_{LAI} in primary human PBL cells (EC_{50}>100 µM; CC_{50}>100 µM).

The antiviral spectrum of RTZ

The antiviral effects exerted by RTZ on HIV-1_{LAI} and HCV-1b Con1 were confirmed and extended by data including HBV subtype ayw (HBV ayw; Figure 2A), HHV-6B strain Z29, HHV-8 strain BCBL-1 and wild-type EBOV Zaire 1976 Mayinga (Table 1). Additionally, the antiviral spectrum of RTZ was assessed versus 26 virus species from differently selected RNA and DNA virus families towards which RTZ was found to be inactive (*Assessing the antiviral spectrum of RTZ* in

Figure 2. The established GRE 1 and the putative GRE 2 in the 3,182 nucleotide partially double-stranded DNA genome of HBV subtype ayw

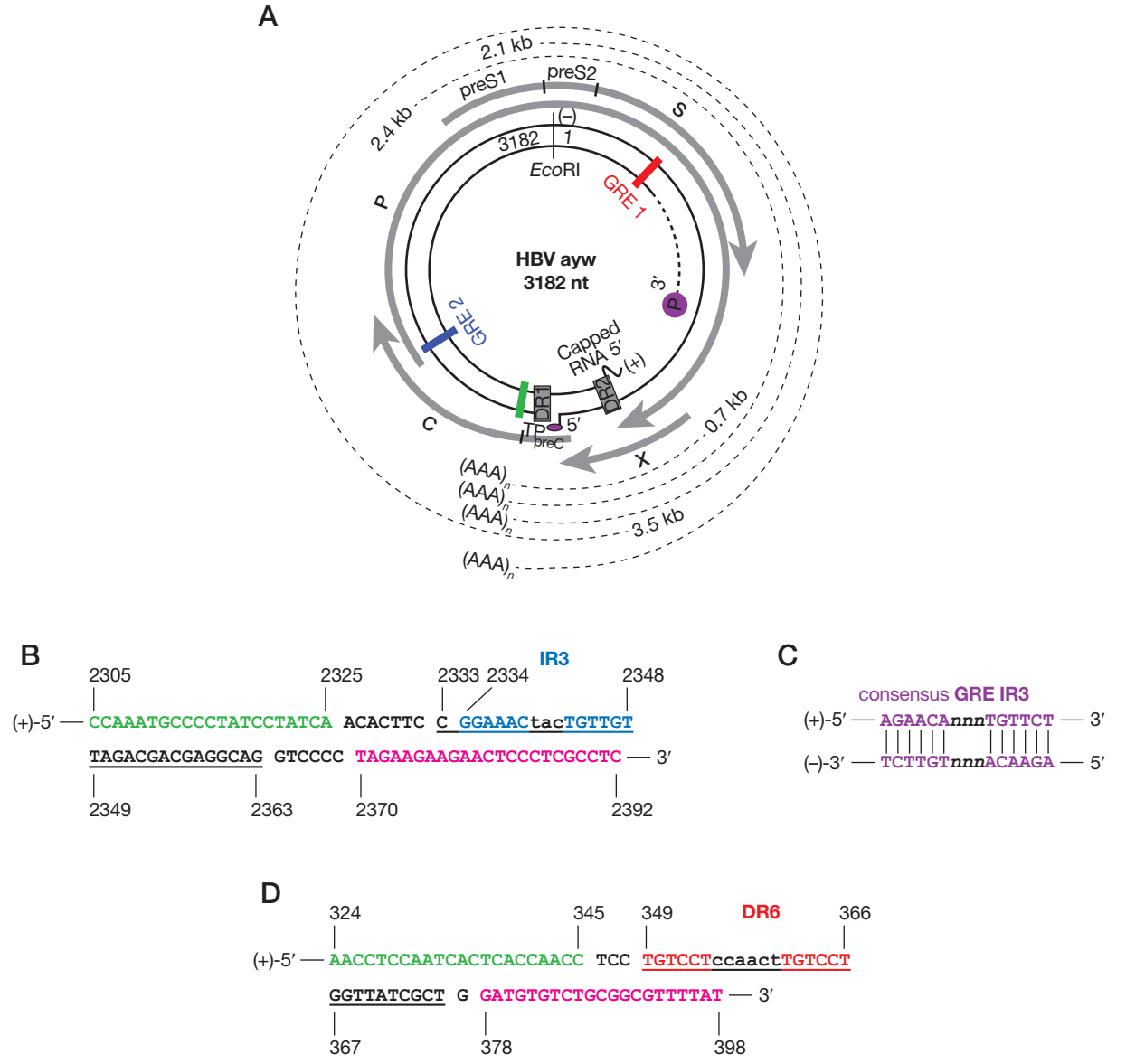

(A) HBV ayw genome chart with glucocorticoid response *cis*-element (GRE) 1 (in red) and GRE 2 (in blue), the unique *Eco*RI restriction site, direct repeat 1 (DR1) and DR2, the 3′-liganded HBV polymerase (P, in purple), the 5′-covalently attached terminal protein (TP, in purple), the polyadenylation signal sequence (in green), the four HBV mRNA transcripts (3.5 kb, 2.4 kb, 2.1 kb, 0.7 kb), the HBV mRNA poly-A tails ($[AAA]_n$), and the capped RNA primer of the incomplete (+)-strand. **(B)** The putative intragenomic GRE 2 inverted repeat 3 (IR3; in blue) between nucleotide (nt) 2,334 and 2,348, targeted by TaqMan® real-time quantitative PCR (RT-qPCR) for HBV DNA detection. The forward primer (in green), the reverse primer (in magenta) and the TaqMan® probe (underlined) are shown. **(C)** The (idealized) palindromic consensus GRE inverted repeat 3 (IR3) [43]. **(D)** The established [44,45] dexamethasone-responsive intragenomic GRE 1 direct repeat 6 (DR6; in red) between nt 349 and 366, targeted by TaqMan® RT-qPCR for HBV DNA detection [24]. The forward primer (in green), the reverse primer (in magenta) and the TaqMan® probe (underlined) are shown.

Additional file 1). In detail, RTZ was inactive versus *Picornaviridae*, *Flaviviridae*, *Togaviridae*, *Coronaviridae*, *Rhabdoviridae*, *Paramyxoviridae*, *Arenaviridae*, *Bunyaviridae* and *Orthomyxoviridae*, all of which represent RNA viruses. RTZ was also inactive versus *Adenoviridae*, *Polyomaviridae* and *Poxviridae*, all of which represent DNA viruses. Inactivity of RTZ was additionally detected towards HHV-1 (herpes simplex virus type 1), HHV-2 (herpes simplex virus type 2) and HHV-4 (Epstein–Barr virus).

Table 1. Antiviral *in vitro* activities of RTZ

Virus	Virus strain	Cell line	Assay type	EC_{50} and/or (EC_{90})	CC_{50}	SI_{50} and/or (CC_{50}/EC_{90})	EC_{50} and/or (EC_{90})	CC_{50}	SI_{50} and/or (CC_{50}/EC_{90})
EBOV Zaire	1976 Mayinga (wild-type)	Vero	VYR	(10)[a]	100[a]	(10)[a]	(1,100)[b]	3,700[b]	(3.4)[b]
HIV-1	LAI	PBL cells	RT [5α-^{3}H]dTTP	3.61 ±2.47 (30.57 ±24.60)[c]	>100×10^3[c]	>27.7×10^3 (>3,270)[c]	4.07 ±1.80 (16.77 ±5.47)[d]	22.70 ±9.36[d]	5.6 (1.4)[d]
HBV	ayw	HepG2 2.2.15	[^{32}P]DNA hybridization	45[e]	2,255×10^3[e]	50.11×10^3[e]	>100[f]	24[f]	<0.2[f]
			TaqMan® RT-qPCR	5[e]	>100[e]	>20[e]	5.0[f]	17.3[f]	3.5[f]
HCV-1b	Con1	Huh7 ET (luc-ubi-neo/ET) replicon	Luciferase reporter	0.07 (0.27)[g]	>2[g]	>28.6 (>7.4)[g]	260 (630)[h]	5,024[h]	19.3 (8.0)[h]
			TaqMan® RT-qPCR	0.15 (1.21)[g]	>2[g]	>13.3 (>1.7)[g]	360 (1,970)[h]	11.17×10^3[h]	31.0 (5.7)[h]
HHV-6B	Z29	MOLT-3	DIG-DNA hybridization	9.2 (23.0)[i]	88.2[i]	9.6 (3.8)[i]	3.3 (10.3)[j]	41.9[j]	12.7 (4.1)[j]
HHV-8 (KSHV)	BCBL-1	BCBL-1 (KSHV producer cells)	TaqMan® RT-qPCR	9.2 (>60)[k]	>60[k]	>6.5[k]	11.1 (>12)[l]	41.7[l]	3.8 (<3.5)[l]

BCBL-1, body cavity-based lymphoma-1 cells; CC_{50}, host cellular (cyto)toxic concentration 50%; DIG-DNA, digoxigenin-labelled DNA probe; EBOV Zaire, Ebola virus Zaire; EC_{50}, effective concentration 50%; EC_{90}, effective concentration 90%; SI_{50}, selectivity index 50% (=CC_{50}/EC_{50}); HepG2 2.2.15, human hepatocellular carcinoma (HCC) HBV ayw producer cells; HHV-6B, human herpesvirus 6 type B; HHV-8, human herpesvirus 8; hrIFN-α2b, human recombinant interferon-α2b (*M*=19,271 g/mol; activity 2.6×10^8 IU/mg; 1 IU corresponds to 3.85 pg hrIFN-α2b, 1 IU/ml to 200 fM hrIFN-α2b protein concentration); Huh7 ET (luc-ubi-neo/ET) replicon, subgenomic HCV-1b RNA replicon cell line; KSHV, Kaposi's sarcoma-associated herpesvirus; PBL cells, primary human peripheral blood lymphocyte cells; MOLT-3, acute lymphoblastic leukaemia T lymphoblast cell line; RT, reverse transcriptase; TaqMan® RT-qPCR, TaqMan® real-time quantitative polymerase chain reaction; Vero, African green monkey (grivet) *Chlorocebus aethiops* (syn. *Cercopithecus aethiops*) kidney epithelial cells; VYR, virus yield reduction; [^{32}P]DNA, phosphorus-32-labelled DNA probe; [5α-^{3}H]dTTP, 5α-tritiated thymidine 5′-triphosphate. [a]3-Deazaguanine, μM. [b]Retinazone (RTZ), nM. [c]Zidovudine (AZT), nM ±SD, *n*=14, r^2=0.97. [d]RTZ, μM ±SD, *n*=6, r^2=0.98. [e](–)-lamivudine, nM. [f]RTZ, μM. [g]hrIFN-α2b, IU/ml. [h]RTZ, nM. [i]Cidofovir (CDV), μM. [j]RTZ, μM. [k]CDV, μM. [l]RTZ, μM.

The differential effects of RTZ on HBV ayw

Interestingly, we found antiviral activity of RTZ (EC_{50}=5.0 μM) on HBV ayw only in the quantitative polymerase chain reaction (qPCR) assay, whereas in the Southern blot DNA hybridization assay we could not detect antiviral activity of RTZ. The difference between the two assays is that in qPCR a TaqMan® real-time qPCR (TaqMan® RT-qPCR) probe was used with suitable forward and reverse primers, whereas in the DNA hybridization assay a 3.2 kb *Eco*RI-digested full-genomic (Figure 2A) ^{32}P-labelled HBV DNA probe [23] was applied. Therefore, we conclude that HBV DNA was fully produced in the presence of RTZ, but was not functional (that is, not functional as readable template). This means that RTZ must have covalently modified the HBV DNA in the sequence region complementary to the TaqMan® RT-qPCR probe. The qPCR probe utilized spanned from nucleotide (nt) 2,333 to nt 2,363 of HBV ayw DNA (Figure 2B). In this region we identified a good putative glucocorticoid nuclear receptor (GR) response DNA *cis*-element (glucocorticoid response element [GRE]) inverted repeat 3 (IR3), **GGAAAC**tac**TGTTGT** (GRE 2; Figure 2B). The standard GRE consensus sequence is the IR3, **AGAACA***nnn***TGTTCT** (Figure 2C) [43]. The putative GRE 2 is obviously better than the GRE 1 direct repeat 6 (DR6) identified by Tur-Kaspa *et al*. [44,45] between nt 349 and nt 366, **TGTCCT**ccaact**TGTCCT** (Figure 2D; bold and underlined sequence = nuclear receptor-binding half-site DNA sequence). Interestingly, a HBV ayw DNA-detecting TaqMan® RT-qPCR was published by Morrey *et al*. [24] with the probe sequence located between nt 349 and nt 376, that is starting with the first nucleotide of GRE 1.

The covalent modification of λ bacteriophage DNA by RTZ

To verify the reaction of RTZ with DNA, the covalent modification of λ bacteriophage double-stranded DNA (dsDNA) by RTZ under catalysis of aqueous acetic acid (HOAc) at room temperature (RT) was examined. Firstly, without HOAc no reaction was observed at RT (*Covalent modification of λ DNA by RTZ* in Additional file 1) or 70°C (*Covalent modification of λ DNA by RTZ* in Additional file 1), indicating that RTZ is non-mutagenic under these conditions. Secondly, under HOAc catalysis production of hydrazinothiocarbonyl-DNA (HTC-DNA) was observed as detected by thin-layer chromatography (TLC; *Covalent modification of λ DNA by RTZ* in Additional file 1). The acid-sensitive by-product all-*trans* retinal (vitamin A–aldehyde) was degraded by HOAc to OBH acetate. Oligomeric λ dsDNA was de-polymerized and reacted with (5*RS*)-5-(14-apo-β-caroten-14-yl)-1,3,4-oxadiazolidine-2-thione (ACO) by *trans*-thiocarbamoylation of its lact(hi)one ring. ACO is formed by splitting of RTZ under HOAc catalysis into the components (2*E*)-2-(all-*trans* retinylidene)hydrazinecarbothioic *O*-acid (which spontaneously cyclized to ACO) and (15*E*)-all-*trans* retinal thiosemicarbazone (ATR-TSC; *Splitting of RTZ by acid catalysis* in Additional file 1). The ATR-TSC was isolated from HOAc-treated RTZ and identified by NMR spectroscopy (see Additional file 1). These elucidations suggest that RTZ can modify viral target DNA (*Covalent modification of HBV subtype ayw DNA by RTZ* in Additional file 1) under proton catalysis. A direct (covalent) binding of RTZ to the glucocorticoid hydrocortisone could be excluded by investigating the chemical reaction of RTZ with hydrocortisone in aqueous ethanol at elevated temperature under presence of HOAc. Only ATR-TSC in admixture with OBH acetate could be isolated (see Additional file 1). This pointed to chemical inertness of hydrocortisone towards RTZ.

The mechanism of the anti-HBV ayw activity exerted by RTZ

The anti-HBV effect of RTZ should be mediated by GR, since the HBV genome contains at least two GR *trans*-activation targets (GREs). We propose that RTZ binds to human GR (hGR), is transported through the nuclear pore complex [46] to the intranuclear HBV genome by the RTZ-liganded hGR, the RTZ–hGR complex binds to GREs, and, finally, the co-transported RTZ switches to the HBV DNA and covalently modifies amine group-containing nucleobases (cytosine, guanine, adenine) by *trans*-thiocarbamoylation (*Splitting of RTZ by acid catalysis* and *Covalent modification of HBV subtype ayw DNA by RTZ* in Additional file 1). This could also happen for host cellular GREs, but we think there is selectivity for intraexonic GREs, which are not typical for the human genome [47], because viral intraexonic GREs are subject to different epigenetic regulation involving chromatin remodelling events [48] in comparison to host cellular GREs [47,48]. Human GREs are located in the promoter regions upstream of transcription initiation sites [47], with only few exceptions where the GRE is found within a human gene intron [49]. Additionally, it should be mentioned that human GREs are in most instances imperfect (GRE sequence degeneracy), that is, their sequences do not match the perfect GRE consensus sequence given (Figure 2C) [50]. In spite of these imperfect GRE sites, their glucocorticoid responsiveness is retained [47,50]. The linearized, full-genomic 3.2 kb HBV DNA probe could have hybridized to the RTZ-modified HBV DNA because two mutant nucleotides (in GRE 2) out of 3,182 are too minimal in extent (0.6285‰) to prevent hybridization.

The anti-HIV-1_{LAI} activity of RTZ

For the case of HIV-1_{LAI} a striking analogy to HBV ayw is predicted. HIV-1_{LAI} proviral DNA (*The proviral DNA genome of HIV-1_{LAI}* in Additional file 1) contains four recognized GREs (GRE 1, GRE 2, GRE 3 and GRE 4) [51]. GRE 1 (-264 to -259), GRE 2 (-6 to -1) and GRE 3 (+15 to +20) are located within the 5′-long terminal repeat (5′-LTR) [52] (*The proviral DNA genome of HIV-1_{LAI}* in Additional file 1). The GRE 4, **AGGACA**tat**AGTTAG**, is located in the *vif* coding exon from nt 4,997 to nt 5,011 [53], and is both intragenic and intraexonic (bold and underlined sequence = nuclear receptor-binding half-site DNA sequence; *The proviral DNA genome of HIV-1_{LAI}* in Additional file 1). This GRE 4 is proposed as a target of RTZ, since the 5′-LTR GREs are only partially functional negative enhancers (silencers) of HIV-1 gene expression, whereas the GRE 4 in the *vif* gene was shown to be fully functional as enhancer of HIV gene transcription [53]. The covalent modification of HIV-1_{LAI} *vif* gene by RTZ, in close analogy to the already described mechanism-of-action on HBV ayw, would lead to loss of HIV-1_{LAI} Vif protein (Vif = viral infectivity factor) function. Vif protein serves as an inherent retroviral inhibitor of the innate human apolipoprotein B mRNA-editing enzyme 3G (APOBEC3G)-dependent human antiretroviral defense system [54]. As a consequence, Vif could not protect HIV-1 (–)-cDNA against host APOBEC3G cytidine deaminase enzymatic activity (dC→dU mutation). This mechanism could have happened in the PBL cells used for our HIV-1_{LAI} assays, since PBL cells are non-permissive for Vif-deficient HIV-1 due to constitutive expression of APOBEC3G [54].

Correlation of the antiviral spectrum of RTZ with the presence of viral GREs

Evidence for an involvement of human GR and its corresponding GREs in the antiviral activity spectrum of RTZ provided the comparison of complete genome data of RTZ-susceptible and RTZ-insensitive viruses with DNA stage (Table 2). In a systematic computational complete genome search all available RTZ-susceptible and RTZ-insensitive virus genomes were examined for intraexonic GREs of the consensus GRE type (Figure 2C), the HIV-1_{LAI} *vif* GRE-related type, and the HBV ayw GRE 2-related type (Table 2). The GRE hits clearly indicated that in all RTZ-susceptible virus genomes at least one GRE was found within a gene essential for *in vitro* virus replication, whereas in all RTZ-insensitive virus genomes no GRE was found in genes essential for *in vitro* virus replication (Table 2).

In detail, the essentiality (indispensable function) or non-essentiality (dispensable function) of the gene(s) which contain the intragenic/intraexonic GRE elements for *in vitro* replication of the virus is indicated in Table 2. Included in the search algorithm were the consensus GRE **AG(A/G)ACA**nnn**TGT(T/C)CT**, the HIV-1_{LAI} *vif*-GRE-related 5′-half-site **AG(A/G)ACA**, the HBV ayw GRE 2-related 5′-half-site **GGAAAC**, and the 3′-half-sites **AG(T/C)(T/C)N(T/G/A)** or **TG(T/G/C)(T/G/C)N(T/A)** (n and N both stand for any nucleotide). Excluded were the repeats **CCC, GGGG, TTT** and **TTTT** in the sequences, and hits in non-functional intron and hypothetical (unknown) protein sequences (bold and underlined sequence = nuclear receptor-binding half-site DNA sequence). The HIV-1_{LAI} *vif* gene essentiality is cell type-dependent. RTZ was tested in *vif*-deletion mutant non-permissive PBL cells [54]. The varicella-zoster virus ORF52 helicase–primase complex primase subunit [55], the HCMV U_L49 (HFLF5) tegument protein VP22 [56], the HHV-6B U38 DNA-dependent DNA polymerase (DNA pol) [57] and the KSHV ORF9 DNA-dependent DNA polymerase [58] are essential for *in vitro* virus replication. The HCMV U_L47 capsid assembly protein (component of the tegument) [59] and the HHV-6B U69 kinase/phosphotransferase (ganciclovir kinase) [34,60] are of intermediate *in vitro* essentiality. The HCMV U_S15 (HVLF3) protein [61], the herpes simplex virus type 1 U_L10 transmembrane glycoprotein M (*g*M) [62] and the Epstein–Barr virus BHRF1 protein, a human Bcl-2 homologue [63], are non-essential for *in vitro* virus replication.

RTZ is a weak glucocorticoid antagonist and binds to human GRα

To obtain verification for the previous postulations, the binding of RTZ to hGR isoform α (hGRα) ligand (steroid)-binding domain (hGRα LBD) was examined (Figure 3). Indeed, RTZ did bind to hGRα LBD as determined by LanthaScreen® time-resolved TR–FRET glucocorticoid receptor coactivator assay. This steroid receptor coactivator-1 (SRC-1) [38] assay decides between agonist or antagonist activity of a test compound at hGRα LBD. RTZ acted as a weak antagonist at hGRα LBD, as compared to the potent hGRα LBD antagonist mifepristone (RU486; Figure 3A). The result was statistically significant ($P<0.01$). Subsequently, the concentration-dependent displacement of the fluorescein-labelled glucocorticoid agonist Fluormone™ GS1 Green from hGRα LBD by RTZ was interpolated to show an EC_{50} of 96 µM, as determined by the LanthaScreen® TR–FRET glucocorticoid receptor competitive binding assay (Figure 3B). The result was statistically significant ($P<0.001$). Therefore, it is reasonable to assume that RTZ binds to hGRα, acting as a weak, but detectable glucocorticoid nuclear receptor antagonist.

Effects of RTZ on EBOV Zaire replication

The inhibition of eGFP–EBOV Zaire 1976 Mayinga multiplication by RTZ was examined in more detail (Figure 4). The EC_{50} of RTZ was interpolated to 830 nM (Figure 4). In comparison, the bis-benzamidine

Table 2. Correlation of the antiviral spectrum of RTZ with the presence of intragenic/intraexonic GRE IR3 elements in RTZ-susceptible viruses

Virus	Virus strain[a]	Virus species RTZ-susceptible *in vitro*?, yes/no (*in vitro* EC_{50})	Complete genome accession number (GenBank or NCBI)	Complete genome base pairs	Gene(s)	Gene(s) essential *in vitro*?, yes/no	GRE IR3 sequence position	GRE IR3 element AG(A/G)ACA or GGAAAC (5′-half-site) and AG(T/C)(T/C)N(T/G/A) or TG(T/G/C)(T/G/C)N(T/A) (3′-half-site) and excluding CCC, GGGG, TTT and TTTT
HBV	ayw	Yes (5.0 µM)	GenBank U95551.1	3,182	C(ore), P(ol)	Yes	2,334–2,348	GGAAACtacTGTTGT
HIV-1	LAI (BRU, LAV-1)	Yes (4.1 µM)	GenBank K02013.1	9,229	*vif*	Yes[b]	4,997–5,011	AGGACAtatAGTTAG
VZV (HHV-3)	Dumas	Yes (4.7 µM)	NCBI RefSeq NC_001348.1	124,884	ORF52 primase	Yes	91,533–91,547	GGAAACggaTGGGTT
	NH29_3		GenBank DQ674250.1	124,811			91,462–91,476	
HCMV (HHV-5)	AD169	Yes (2.4 µM)	GenBank X17403.1	229,354	U_S15 (HVLF3)	No	204,108–204,122	GGAAACggcTGCTCT
					U_L47 tegument	Yes/No	63,268–63,282	AGGACAtctTGTCTT
					U_L49 (HFLF5)	Yes	70,912–70,926	AGAACAtcgAGTTGA
HHV-6B	Z29	Yes (3.3 µM)	NCBI RefSeq NC_000898.1	162,114	U2 *trans*-activator	Unknown	10,341–10,355	GGAAACttcTGCGAA
					U33 capsid	Unknown	53,268–53,282	AGAACAtggAGCTCA
							53,386–53,400	AGAACAtttAGTCTT
					U69 kinase	Yes/No	105,528–105,542	GGAAACtggAGCTAG
					U38 DNA pol	Yes	58,212–58,226	AGAACAacaAGTCCA
KSHV (HHV-8)	GK18	Yes (11.1 µM)	NCBI RefSeq NC_009333.1	137,969	ORF9 DNA pol	Yes	12,802–12,816	GGAAACtacTGTGTT
	BC-1		GenBank U75698.1	137,508			12,836–12,850	
HSV-1 (HHV-1)	KOS	No	GenBank JQ780693.1	151,024	U_L10 (*g*M)	No	23,288–23,302	GGAAACgtcTGCTCT
	17		NCBI RefSeq NC_001806.1	152,261			23,630–23,644	
	H129		GenBank GU734772.1	152,066			23,587–23,601	GGAAACgtcTGTTCT
HSV-2 (HHV-2)	HG52	No	NCBI RefSeq NC_001798.1	154,746	–	–	–	No GRE detectable (according to defined search criteria)
EBV (HHV-4) type 1	B95-8	No	NCBI RefSeq NC_007605.1	171,823 (circular)	BHRF1	No	42,424–42,438	AGGACAttgTGTTGT
EBV (HHV-4) type 2	AG876		NCBI RefSeq NC_009334.1	172,764 (circular)			42,540–42,554	

EBV, Epstein–Barr virus; EC_{50}, effective concentration 50%; GRE, glucocorticoid response element; HCMV, human cytomegalovirus; HHV, human herpesvirus; HSV, herpes simplex virus; KSHV, Kaposi's sarcoma-associated herpesvirus; NCBI RefSeq, National Center for Biotechnology Information (NCBI) Reference Sequence; VZV, varicella-zoster virus. [a]The given virus strain is not necessarily the one tested for RTZ-susceptibility, but was selected with respect to availability of complete genome sequence data. [b]The *in vitro* essentiality of HIV-1 *vif* is strongly cell type-dependent.

Table 2. Continued

Virus	Virus strain[a]	Virus species RTZ-susceptible *in vitro*?, yes/no (*in vitro* EC_{50})	Complete genome accession number (GenBank or NCBI)	Complete genome base pairs	Gene(s)	Gene(s) essential *in vitro*?, yes/no	GRE IR3 sequence position	GRE IR3 element AG(A/G)ACA or GGAAAC (5′-half-site) and AG(T/C)(T/C)N(T/G/A) or TG(T/G/C)(T/G/C)N(T/A) (3′-half-site) and excluding CCC, GGGG, TTT and TTTT
Human adenovirus A	HAdV-12 (Huie)	No	NCBI RefSeq NC_001460.1	34,125	–	–	–	No GRE detectable (according to defined search criteria)
Human adenovirus B	HAdV-3 (GB)		NCBI RefSeq NC_011203.1	35,343	–	–	–	
Human BK polyomavirus	Dunlop	No	NCBI RefSeq NC_001538.1	5,153 (circular)	–	–	–	
Vaccinia virus	Copenhagen	No	GenBank M35027.1	191,737	–	–	–	
Cowpox virus	Brighton Red	No	NCBI RefSeq NC_003663.2	224,499	–	–	–	
Monkeypox virus	MPXV-USA-2003-044	No	GenBank DQ011153.1	198,780	–	–	–	

Figure 3. RTZ represents a weak glucocorticoid antagonist

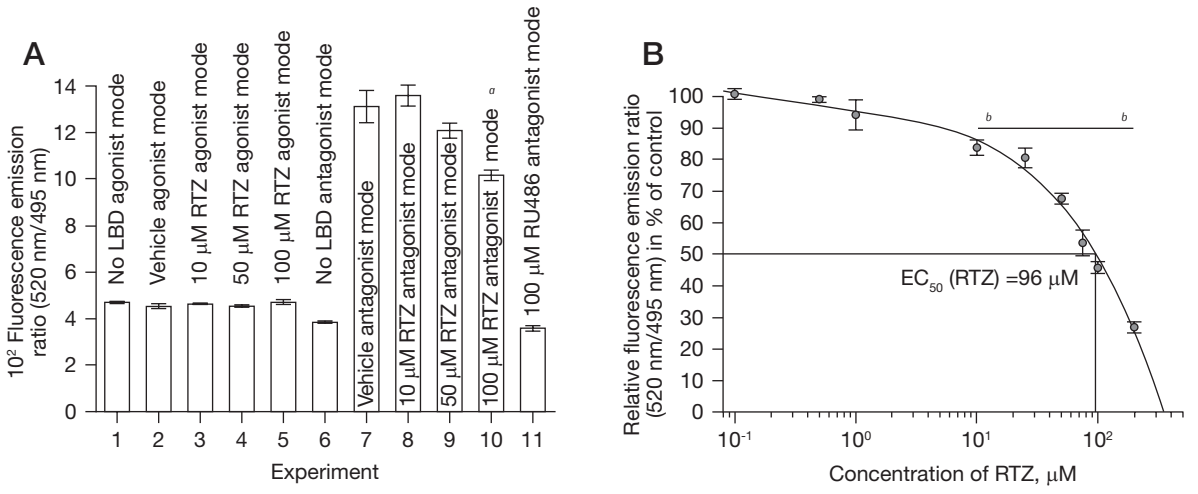

(A) The LanthaScreen® TR–FRET glucocorticoid receptor coactivator assay performed with retinazone (RTZ). The assay discriminates whether a test compound acts as an agonist or antagonist at human glucocorticoid receptor isoform α ligand-binding domain (hGRα LBD). Experiments 1–5 were run in agonist mode, experiments 6–11 in antagonist mode. RTZ behaved as a weak hGRα LBD antagonist in comparison to the potent hGRα LBD antagonist mifepristone (RU486). Vehicle control was 1% DMSO in TR–FRET nuclear receptor buffer F, for which the assay was validated. Error bars are mean ±SEM, n=3. **(B)** The LanthaScreen® TR–FRET glucocorticoid receptor competitive binding assay performed with RTZ. The effective concentration 50% (EC_{50}=96 μM) for the concentration-dependent displacement of the fluorescein-labelled glucocorticoid agonist Fluormone™ GS1 Green from hGRα LBD by RTZ was interpolated with SigmaPlot® 11.0 (Systat Software, Inc., San Jose, CA, USA, 2008). The vehicle control (0% agonist displacement level) included 20 nM agonist and 1% DMSO in TR–FRET nuclear receptor buffer F, for which the assay was validated. The 100% displacement level was defined by including 20 μM dexamethasone. Error bars are mean ±SEM, n=3. ^aP<0.01 when compared to control. ^bP<0.001 when compared to controls.

Figure 4. Inhibition of eGFP–EBOV Zaire 1976 Mayinga multiplication by RTZ

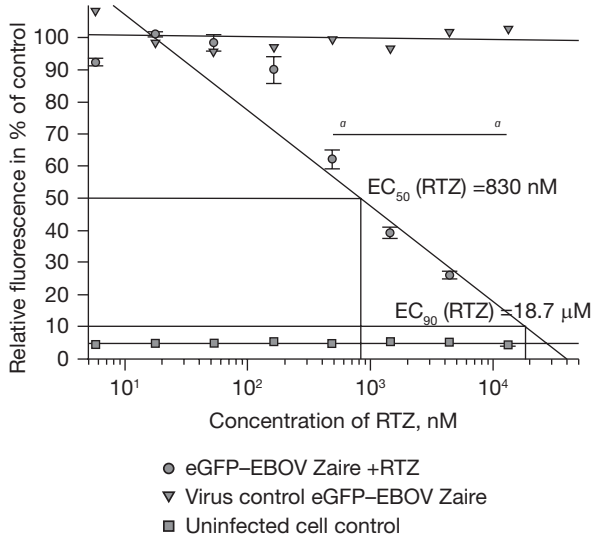

The effect of retinazone (RTZ) on enhanced green fluorescent protein-expressing Ebola virus Zaire (eGFP–EBOV) 1976 Mayinga multiplication in Vero E6 cells (eGFP–EBOV Zaire +RTZ) as measured by detecting eGFP fluorescence, in comparison to the positive control (virus control eGFP–EBOV Zaire, no compound). The background fluorescence negative control (uninfected cell control, no compound) was included. Error bars are mean ±SEM, n=3. Linear regression lines were computed with SigmaPlot® 11.0 (for eGFP–EBOV Zaire +RTZ: r^2=0.8735). The effective concentration 50% (EC_{50}) of RTZ was interpolated (SigmaPlot® 11.0) to 830 nM, and the corresponding effective concentration 90% (EC_{90}) to 18.7 μM. ^aP<0.001 when compared to controls.

small molecule FGI-103 [64] was reported to suppress eGFP–EBOV Zaire 1976 Mayinga recombinant virus multiplication with an EC_{50} of 3.8 μM [64], and to suppress wild-type EBOV Zaire 1976 Mayinga virus yield with an EC_{50} of 100 nM [64]. Because EBOV inhibitors are rather scarce (*Reported* Filovirus *inhibitors* in Additional file 1), the activity of RTZ is interpreted to represent a useful result. The host CC_{50} exerted on Vero E6 cells by RTZ was interpolated to 5.67 μM, yielding a selectivity index 50% (SI_{50}=CC_{50}/EC_{50}) of 6.8. Interestingly, non-tumorigenic HepG2 human HCC cells were completely insensitive to RTZ-mediated toxicity at 13.2 μM concentration, whereas Vero E6 (Vero 76, clone E6) cells were rather sensitive towards RTZ-mediated cellular toxicity, as will be discussed. To verify the results with eGFP–EBOV Zaire 1976 Mayinga recombinant virus, the suppression of wild-type EBOV Zaire 1976 Mayinga virus yield by RTZ was examined in Vero cells. The virus yield was suppressed by RTZ with an effective concentration 90% (EC_{90}) of 1,100 nM (Table 1). The CC_{50} exerted on Vero cells by RTZ was determined to be 3,700 nM by the neutral red method, confirming the high sensitivity of Vero-type cells towards RTZ. The corresponding EC_{50} of RTZ regarding suppression of wild-type EBOV Zaire 1976 Mayinga virus yield could be interpolated to 48.8 nM yielding a SI_{50} of 75.8. Therefore, RTZ is comparable in antifiloviral

potency to FGI-104 and FGI-103 when comparing the suppression of eGFP–EBOV Zaire 1976 Mayinga recombinant virus *in vitro* replication by FGI-104 (EC_{50}=10 µM; CC_{50}>50 µM; SI_{50}>5) [29] and by FGI-103 (EC_{50}=3.8 µM; CC_{50}≥50 µM; SI_{50}≥13.2) [64] with the corresponding data of RTZ (EC_{50}=0.83 µM; CC_{50}=5.67 µM; SI_{50}=6.8). The data of RTZ regarding the *in vitro* suppression of wild-type EBOV Zaire 1976 Mayinga virus yield (EC_{50}=0.0488 µM; CC_{50}=3.7 µM; SI_{50}=75.8) are of compelling evidence for the antifiloviral *in vitro* efficacy of RTZ.

The targeting of the RNA viruses HCV-1b and EBOV Zaire by RTZ

Regarding the antiviral mechanism-of-action of RTZ versus HCV-1b Con1 and EBOV Zaire 1976 Mayinga (*HCV and Ebola virus genomes* in Additional file 1), it is inherently clear that it cannot be being mediated by GRs, since both HCV and EBOV incorporate no DNA stages in their life cycles. It was recently reported that thiosemicarbazones (5,6-dimethoxyindan-1-one thiosemicarbazone) target bovine viral diarrhoea virus type 1 (BVDV-1; strain NADL, *Flaviviridae*, *Pestivirus*) NS5B protein RNA-dependent RNA polymerase [65]. BVDV-1 is commonly regarded as a suitable surrogate for HCV, because both *Flaviviridae* polyprotein sequences are closely related (maximal sequence identity 39%). Because the anti-HCV-1b activity of RTZ was determined with the HCV RNA replicon cell line Huh7 ET (luc-ubi-neo/ET) which only codes for the non-structural HCV proteins NS3, NS4A, NS4B, NS5A and NS5B, the inhibiting action of RTZ must be confined to these five genes and/or gene products.

The toxicity of RTZ on cultured cells

Regarding the toxicity of RTZ on cultured cell lines, the following observations should be added. RTZ (NSC-751959) showed antineoplastic activity within the 60-cancer cell panel included in the Developmental Therapeutics Program of the National Cancer Institute. The RTZ-induced average growth inhibition 50% (GI_{50} ±standard deviation [SD]) was found to be 1.73 ±0.48 µM (*n*=57), the RTZ-induced average growth inhibition 100% (TGI, GI_{100} ±SD) 5.57 ±0.49 µM (*n*=57), and the RTZ-induced average lethal concentration 50% (LC_{50} ±SD, the concentration at which 50% of cells die by apoptosis and/or necrosis) was 19.00 ±0.45 µM (*n*=53) on 57 tested cancer cell lines (*Dose-response graphs of the antineoplastic action of RTZ* and *The experimental analysis of the antineoplastic action of RTZ* in Additional file 1). Therefore, the observed *in vitro* toxicity exerted by RTZ on cultured cells reflects an intrinsic antineoplastic potential which is of considerable interest regarding the oncogenic nature of HIV-1, HBV, HCV and HHV-8. Cell lines especially sensitive to RTZ are, for example, CCRF-CEM (CEM, acute lymphoblastic leukaemia T lymphoblast cells) with a mean CC_{50} (RTZ) ±SD of 1.67 ±0.42 µM (*n*=6), and all Vero cell derivatives (Vero, Vero 76, Vero E6) with a mean CC_{50} (RTZ) ±SD of 5.83 ±4.58 µM (*n*=6) for Vero cells. The primary human PBL cells (containing primary human T lymphocytes) are relatively insensitive towards RTZ with a mean CC_{50} (RTZ) ±SD of 22.70 ±9.36 µM (*n*=6; Table 1).

Discussion

In the case of an infection with HIV-1, current HAART regimens are capable of achieving prolonged suppression of HIV-1 plasma viraemia in HIV-1-infected individuals [66,67]. However, it has not been possible to eradicate HIV-1 through HAART because HIV-1 seems to persist in latent retroviral reservoirs like follicular dendritic $CD4^+$ T-cells located deep within the lymphatic system [66,67]. The mechanism of HIV-1 retroviral latency in persistent reservoirs unamenable to HAART is poorly defined and understood [66,67]. From a theoretical point of view the HIV-1 proviruses integrated in the human host chromatin of latent retroviral reservoirs should be responsible for the severe relapse of HIV-1 viraemia and replication following cessation of HAART in HIV-1-infected patients. By the application of reverse transcription-preceded TaqMan® RT-qPCR assays, the detection of single copies of HIV-1 genomic (+)-ssRNA in small volumes of blood plasma is possible [67]. By this technique it could be shown that low plasma viraemia (*n*<50 HIV-1 genomic RNA copies/ml blood plasma) persists in most HIV-1-infected individuals receiving HAART. It was demonstrated that residual plasma viraemia correlates with the size of the $CD4^+$ T-lymphocyte cell viral reservoir [67], but not with markers of immune activation, suggesting that reactivation of this latent viral reservoir may not be the only source of residual plasma viraemia. This could explain why HIV-1 infection persists even after years of HAART. Although HAART can suppress viral replication greatly, and reduces viraemia to less than 50 HIV-1 genomic RNA copies per ml of blood plasma, proviral latency established within the host genome remains largely unaffected by HAART, and can replenish severe systemic infection following interruption of therapy. Pharmacological strategies which not only target viral replication *per se*, but also deplete proviral host genome infection, are certainly required for successful clearance of HIV-1 infection [66]. Novel therapeutic strategies aimed at targeting the source of residual viraemia are additionally necessary to achieve viral eradication [67].

We have shown that the vitamin A-derived thiosemicarbazone derivative RTZ has the ability to specifically

inactivate human DNA-integrated proviruses of HBV and HIV-1 by exploiting the presence of human glucocorticoid nuclear receptor-binding DNA sequences, the glucocorticoid (hormone receptor) response elements, in the host chromatin-integrated HBV and HIV-1 proviral DNA genomes. These genomes are specifically inactivated by covalent attachment of *N*-HTC moieties to amine group-containing nucleobases (cytosine, guanine, adenine). These HTC-DNA lesions are lethal for the corresponding proviral genome, because they interrupt both DNA replication and RNA transcription from these proviruses. In addition, these lesions probably withstand repair by eukaryotic DNA repair systems like base excision repair [68], and could induce apoptosis in the infected host cell resulting in ultimate clearance of the viral xenogenomes. This opens the profound possibility to cure the blood-borne diseases chronic hepatitis B and AIDS. For the first time a pharmacological intervention could be found, in the form of the vitamin A-derived agent RTZ, which is able to covalently inactivate host chromatin-integrated HBV and HIV-1 proviral DNA genomes. This is a consequence of the affinity of RTZ-liganded human glucocorticoid nuclear receptor to proviral glucocorticoid response elements.

Moreover, HCV and EBOV Zaire, both also causing severe blood-borne human illnesses, are susceptible to life cycle disruption by RTZ. The HCV target of RTZ presumably represents the RNA-dependent RNA polymerase NS5B enzyme protein of HCV, because it carries a common thiosemicarbazone binding site [65]. The EBOV Zaire target of RTZ could be, for example, the filoviral matrix protein VP40. Binding of RTZ to EBOV Zaire proteins is expected to disrupt virus morphogenesis and budding, virion structure and transcriptional regulation of EBOV Zaire. The nanomolar activity of RTZ in inhibiting wild-type EBOV Zaire multiplication points to an efficacious interruption of the life cycle of EBOV Zaire by RTZ.

Regarding the observed *in vitro* toxicity of RTZ, there is evidence that this RTZ-mediated toxicity could be largely reduced *in vivo*, since RTZ is assumed to bind to and be transported with human plasma retinol-binding protein (hRBP) in human blood circulation. The *in vitro* toxicity of RTZ is assumed to be largely a consequence of RTZ interaction with host cellular lipid membranes leading to altered membrane fluidity status [69]. It was reported that *N*-retinylidene amine *Schiff* bases like RTZ bind to the chromophore binding site of hRBP in human blood plasma [70]. It is expected that the RTZ–hRBP *in vivo* complex distributed in human circulation mediates largely reduced toxicity when compared to the direct *in vitro* impact of RTZ on host cells utilized in our present study. Further work is clearly required to clarify this issue.

Acknowledgements

The authors thank T Westfeld, E-M May, D Wiegel and W Wuebbolt (Currenta GmbH & Co. OHG, Leverkusen, Germany) for analytical services. We are deeply indebted to BE Korba (Georgetown University Medical Center, Washington, DC, USA) for conducting the HBV DNA hybridization assay, to GG Olinger and C Scully (US Army Medical Research Institute of Infectious Diseases, Fort Detrick, MD, USA) for performing the eGFP–EBOV experiments, and to CKH Tseng (National Institutes of Health [NIH], National Institute of Allergy and Infectious Diseases [NIAID], Division of Microbiology and Infectious Diseases [DMID], Virology Branch) for supervising the wild-type EBOV experiments. We cordially thank R Koshy (NIH, NIAID, DMID, Enteric and Hepatic Diseases Branch) for helpful discussions. This work was supported in part by NIH CFAR grant 2P30–AI–50409 (to RFS) and by the Department of Veterans Affairs (to RFS). This project has been funded in whole or in part with Federal Funds from the DMID, NIAID, NIH, Department of Health and Human Services, under contract HHSN272201100012I. The Trinity Biomedical Sciences Institute is supported by a capital infrastructure investment from Cycle 5 of the Irish Higher Education Authority's Programme for Research in Third Level Institutions (PRTLI). DKN would like to thank the Irish Research Council and Dell Ireland for funding. LC expressed her thanks to the Health Research Board (HRB/2007/2) for funding. We are obliged to K Hecker (HEKAtech GmbH, Wegberg, Germany) for expert elemental analyses. LC and DKN contributed equally to this work.

Disclosure statement

The authors declare no competing interests.

Additional file

Additional file 1: Supplementary material with all compound characterization data can be found at http://www.intmedpress.com/uploads/documents/0089_Kesel_Additional_file1.pdf.

References

1. Hemelaar J. The origin and diversity of the HIV-1 pandemic. *Trends Mol Med* 2012; **18:**182–192.
2. Marcellin P. Hepatitis B and hepatitis C in 2009. *Liver Int* 2009; **29 Suppl 1:**1–8.
3. Liang TJ, Heller T. Pathogenesis of hepatitis C-associated hepatocellular carcinoma. *Gastroenterology* 2004; **127 Suppl 1:**S62–S71.
4. Beasley RP, Hwang L-Y, Lin C-C, Chien C-S. Hepatocellular carcinoma and hepatitis B virus – a prospective study of 22 707 men in Taiwan. *Lancet* 1981; **318:**1129–1133.

5. Ly KN, Xing J, Klevens RM, Jiles RB, Ward JW, Holmberg SD. The increasing burden of mortality from viral hepatitis in the United States between 1999 and 2007. *Ann Intern Med* 2012; **156:**271–278.
6. Sterling RK. Triple infection with human immunodeficiency virus, hepatitis C virus, and hepatitis B virus: a clinical challenge. *Am J Gastroenterol* 2003; **98:**2130–2134.
7. Dominguez G, Dambaugh TR, Stamey FR, Dewhurst S, Inoue N, Pellett PE. Human herpesvirus 6B genome sequence: coding content and comparison with human herpesvirus 6A. *J Virol* 1999; **73:**8040–8052.
8. Cathomas G. Kaposi's sarcoma-associated herpesvirus (KSHV)/human herpesvirus 8 (HHV-8) as a tumour virus. *Herpes* 2003; **10:**72–77.
9. Feldmann H, Geisbert TW. Ebola haemorrhagic fever. *Lancet* 2011; **377:**849–862.
10. Leroy EM, Kumulungui B, Pourrut X, *et al*. Fruit bats as reservoirs of Ebola virus. *Nature* 2005; **438:**575–576.
11. Kesel AJ. Broad-spectrum antiviral activity including human immunodeficiency and hepatitis C viruses mediated by a novel retinoid thiosemicarbazone derivative. *Eur J Med Chem* 2011; **46:**1656–1664.
12. Wain-Hobson S, Vartanian J-P, Henry M, *et al*. LAV revisited: origins of the early HIV-1 isolates from Institut Pasteur. *Science* 1991; **252:**961–965.
13. Woerz I, Lohmann V, Bartenschlager R. Hepatitis C virus replicons: dinosaurs still in business? *J Viral Hepat* 2009; **16:**1–9.
14. Towner JS, Paragas J, Dover JE, *et al*. Generation of eGFP expressing recombinant Zaire ebolavirus for analysis of early pathogenesis events and high-throughput antiviral drug screening. *Virology* 2005; **332:**20–27.
15. Sanger F, Coulson AR, Hong GF, Hill DF, Petersen GB. Nucleotide sequence of bacteriophage λ DNA. *J Mol Biol* 1982; **162:**729–773.
16. Vizard DL, Ansevin AT. High resolution thermal denaturation of DNA: thermalites of bacteriophage DNA. *Biochemistry* 1976; **15:**741–750.
17. MacHattie LA, Thomas CA, Jr. DNA from bacteriophage lambda: molecular length and conformation. *Science* 1964; **144:**1142–1144.
18. Schinazi RF, Sommadossi J-P, Saalmann V, *et al*. Activities of 3′-azido-3′-deoxythymidine nucleotide dimers in primary lymphocytes infected with human immunodeficiency virus type 1. *Antimicrob Agents Chemother* 1990; **34:**1061–1067.
19. Spira TJ, Bozeman LH, Holman RC, Warfield DT, Phillips SK, Feorino PM. Micromethod for assaying reverse transcriptase of human T-cell lymphotropic virus type III/lymphadenopathy-associated virus. *J Clin Microbiol* 1987; **25:**97–99.
20. Stuyver LJ, Lostia S, Adams M, *et al*. Antiviral activities and cellular toxicities of modified 2′,3′-dideoxy-2′,3′-didehydrocytidine analogues. *Antimicrob Agents Chemother* 2002; **46:**3854–3860.
21. Korba BE, Gerin JL. Use of a standardized cell culture assay to assess activities of nucleoside analogs against hepatitis B virus replication. *Antiviral Res* 1992; **19:**55–70.
22. Stachulski AV, Pidathala C, Row EC, *et al*. Thiazolides as novel antiviral agents. 1. Inhibition of hepatitis B virus replication. *J Med Chem* 2011; **54:**4119–4132.
23. Galibert F, Mandart E, Fitoussi F, Tiollais P, Charnay P. Nucleotide sequence of the hepatitis B virus genome (subtype ayw) cloned in *E. coli*. *Nature* 1979; **281:**646–650.
24. Morrey JD, Korba BE, Beadle JR, Wyles DL, Hostetler KY. Alkoxyalkyl esters of 9-(*S*)-(3-hydroxy-2-phosphonomethoxypropyl)adenine are potent and selective inhibitors of hepatitis B virus (HBV) replication *in vitro* and in HBV transgenic mice *in vivo*. *Antimicrob Agents Chemother* 2009; **53:**2865–2870.
25. Lohmann V, Körner F, Koch J-O, Herian U, Theilmann L, Bartenschlager R. Replication of subgenomic hepatitis C virus RNAs in a hepatoma cell line. *Science* 1999; **285:**110–113.
26. Pietschmann T, Lohmann V, Kaul A, *et al*. Persistent and transient replication of full-length hepatitis C virus genomes in cell culture. *J Virol* 2002; **76:**4008–4021.
27. Ma S, Boerner JE, TiongYip C, *et al*. NIM811, a cyclophilin inhibitor, exhibits potent *in vitro* activity against hepatitis C virus alone or in combination with alpha interferon. *Antimicrob Agents Chemother* 2006; **50:**2976–2982.
28. Hopkins S, Scorneaux B, Huang Z, *et al*. SCY-635, a novel nonimmunosuppressive analog of cyclosporine that exhibits potent inhibition of hepatitis C virus RNA replication *in vitro*. *Antimicrob Agents Chemother* 2010; **54:**660–672.
29. Kinch MS, Yunus AS, Lear C, *et al*. FGI-104: a broad-spectrum small molecule inhibitor of viral infection. *Am J Transl Res* 2009; **1:**87–98.
30. Shurtleff AC, Biggins JE, Keeney AE, *et al*. Standardization of the filovirus plaque assay for use in preclinical studies. *Viruses* 2012; **4:**3511–3530.
31. Cook PD, Rousseau RJ, Mian AM, Dea P, Meyer RB, Jr., Robins RK. Synthesis of 3-deazaguanine, 3-deazaguanosine, and 3-deazaguanylic acid by a novel ring closure of imidazole precursors. *J Am Chem Soc* 1976; **98:**1492–1498.
32. Repetto G, del Peso A, Zurita JL. Neutral red uptake assay for the estimation of cell viability/cytotoxicity. *Nat Protoc* 2008; **3:**1125–1131.
33. Williams-Aziz SL, Hartline CB, Harden EA, *et al*. Comparative activities of lipid esters of cidofovir and cyclic cidofovir against replication of herpesviruses *in vitro*. *Antimicrob Agents Chemother* 2005; **49:**3724–3733.
34. Prichard MN, Frederick SL, Daily S, *et al*. Benzimidazole analogs inhibit human herpesvirus 6. *Antimicrob Agents Chemother* 2011; **55:**2442–2445.
35. Prichard MN, Daily SL, Jefferson GM, Perry AL, Kern ER. A rapid DNA hybridization assay for the evaluation of antiviral compounds against Epstein-Barr virus. *J Virol Methods* 2007; **144:**86–90.
36. James SH, Hartline CB, Harden EA, *et al*. Cyclopropavir inhibits the normal function of the human cytomegalovirus UL97 kinase. *Antimicrob Agents Chemother* 2011; **55:**4682–4691.
37. Prichard MN, Quenelle DC, Hartline CB, *et al*. Inhibition of herpesvirus replication by 5-substituted 4′-thiopyrimidine nucleosides. *Antimicrob Agents Chemother* 2009; **53:**5251–5258.
38. Oñate SA, Tsai SY, Tsai M-J, O'Malley BW. Sequence and characterization of a coactivator for the steroid hormone receptor superfamily. *Science* 1995; **270:**1354–1357.
39. Jung-Testas I, Baulieu E-E. Inhibition of glucocorticosteroid action in cultured L-929 mouse fibroblasts by RU 486, a new anti-glucocorticosteroid of high affinity for the glucocorticosteroid receptor. *Exp Cell Res* 1983; **147:**177–182.
40. Kesel AJ, Sonnenbichler I, Polborn K, *et al*. A new antioxidative vitamin B_6 analogue modulates pathophysiological cell proliferation and damage. *Bioorg Med Chem* 1999; **7:**359–367.
41. Mascal M, Hafezi N, Meher NK, Fettinger JC. Oxatriquinane and oxatriquinacene: extraordinary oxonium ions. *J Am Chem Soc* 2008; **130:**13532–13533.
42. Mascal M, Hafezi N, Toney MD. 1,4,7-Trimethyloxatriquinane: S_N2 Reaction at tertiary carbon. *J Am Chem Soc* 2010; **132:**10662–10664.
43. Mangelsdorf DJ, Thummel C, Beato M, *et al*. The nuclear receptor superfamily: the second decade. *Cell* 1995; **83:**835–839.
44. Tur-Kaspa R, Burk RD, Shaul Y, Shafritz DA. Hepatitis B virus DNA contains a glucocorticoid-responsive element. *Proc Natl Acad Sci U S A* 1986; **83:**1627–1631.
45. Tur-Kaspa R, Shaul Y, Moore DD, *et al*. The glucocorticoid receptor recognizes a specific nucleotide sequence in hepatitis B virus DNA causing increased activity of the HBV enhancer. *Virology* 1988; **167:**630–633.
46. Vandevyver S, Dejager L, Libert C. On the trail of the glucocorticoid receptor: into the nucleus and back. *Traffic* 2012; **13:**364–374.

47. Schoneveld OJLM, Gaemers IC, Lamers WH. Mechanisms of glucocorticoid signalling. *Biochim Biophys Acta* 2004; **1680:**114–128.
48. George AA, Schiltz RL, Hager GL. Dynamic access of the glucocorticoid receptor to response elements in chromatin. *Int J Biochem Cell Biol* 2009; **41:**214–224.
49. Slater EP, Rabenau O, Karin M, Baxter JD, Beato M. Glucocorticoid receptor binding and activation of a heterologous promoter by dexamethasone by the first intron of the human growth hormone gene. *Mol Cell Biol* 1985; **5:**2984–2992.
50. Horie-Inoue K, Takayama K, Bono HU, Ouchi Y, Okazaki Y, Inoue S. Identification of novel steroid target genes through the combination of bioinformatics and functional analysis of hormone response elements. *Biochem Biophys Res Commun* 2006; **339:**99–106.
51. Pereira LA, Bentley K, Peeters A, Churchill MJ, Deacon NJ. A compilation of cellular transcription factor interactions with the HIV-1 LTR promoter. *Nucleic Acids Res* 2000; **28:**663–668.
52. Mitra D, Sikder SK, Laurence J. Role of glucocorticoid receptor binding sites in the human immunodeficiency virus type 1 long terminal repeat in steroid-mediated suppression of HIV gene expression. *Virology* 1995; **214:**512–521.
53. Soudeyns H, Geleziunas R, Shyamala G, Hiscott J, Wainberg MA. Identification of a novel glucocorticoid response element within the genome of human immunodeficiency virus type 1. *Virology* 1993; **194:**758–768.
54. Marin M, Rose KM, Kozak SL, Kabat D. HIV-1 Vif protein binds the editing enzyme APOBEC3G and induces its degradation. *Nat Med* 2003; **9:**1398–1403.
55. Chono K, Katsumata K, Kontani T, *et al*. ASP2151, a novel helicase–primase inhibitor, possesses antiviral activity against varicella–zoster virus and herpes simplex virus types 1 and 2. *J Antimicrob Chemother* 2010; **65:**1733–1741.
56. Zhang W, Li H, Li Y, *et al*. Effective inhibition of HCMV UL49 gene expression and viral replication by oligonucleotide external guide sequences and RNase P. *Virol J* 2010; **7:**100.
57. Bonnafous P, Boutolleau D, Naesens L, Deback C, Gautheret-Dejean A, Agut H. Characterization of a cidofovir-resistant HHV-6 mutant obtained by *in vitro* selection. *Antiviral Res* 2008; **77:**237–240.
58. Chen Y, Ciustea M, Ricciardi RP. Processivity factor of KSHV contains a nuclear localization signal and binding domains for transporting viral DNA polymerase into the nucleus. *Virology* 2005; **340:**183–191.
59. Bechtel JT, Shenk T. Human cytomegalovirus UL47 tegument protein functions after entry and before immediate-early gene expression. *J Virol* 2002; **76:**1043–1050.
60. Kuny CV, Chinchilla K, Culbertson MR, Kalejta RF. Cyclin-dependent kinase-like function is shared by the beta- and gamma- subset of the conserved herpesvirus protein kinases. *PLoS Pathog* 2010; **6:**e1001092.
61. Mockenhaupt T, Reschke M, Bogner E, Reis B, Radsak K. Structural analysis of the US-segment of a viable temperature sensitive human cytomegalovirus mutant. *Arch Virol* 1994; **137:**161–169.
62. Baines JD, Roizman B. The open reading frames U_L3, U_L4, U_L10, and U_L16 are dispensable for the replication of herpes simplex virus 1 in cell culture. *J Virol* 1991; **65:**938–944.
63. Lee M-A, Yates JL. BHRF1 of Epstein-Barr virus, which is homologous to human proto-oncogene *bcl2*, is not essential for transformation of B cells or for virus replication *in vitro*. *J Virol* 1992; **66:**1899–1906.
64. Warren TK, Warfield KL, Wells J, *et al*. Antiviral activity of a small-molecule inhibitor of filovirus infection. *Antimicrob Agents Chemother* 2010; **54:**2152–2159.
65. Castro EF, Fabian LE, Caputto ME, *et al*. Inhibition of bovine viral diarrhea virus RNA synthesis by thiosemicarbazone derived from 5,6-dimethoxy-1-indanone. *J Virol* 2011; **85:**5436–5445.
66. Choudhary SK, Margolis DM. Curing HIV: pharmacologic approaches to target HIV-1 latency. *Annu Rev Pharmacol Toxicol* 2011; **51:**397–418.
67. Chun T-W, Murray D, Justement JS, *et al*. Relationship between residual plasma viremia and the size of HIV proviral DNA reservoirs in infected individuals receiving effective antiretroviral therapy. *J Infect Dis* 2011; **204:**135–138.
68. Germann MW, Johnson CN, Spring AM. Recognition of damaged DNA: structure and dynamic markers. *Med Res Rev* 2012; **32:**659–683.
69. Meeks RG, Zaharevitz D, Chen RF. Membrane effects of retinoids: possible correlation with toxicity. *Arch Biochem Biophys* 1981; **207:**141–147.
70. Horwitz J, Heller J. Properties of the chromophore binding site of retinol-binding protein from human plasma. *J Biol Chem* 1974; **249:**4712–4719.

Received 5 February 2013; accepted 22 March 2013; published online 2 May 2013